

Temperature and doping dependent flat-band superconductivity on the Lieb-lattice

Feng Xu(徐峰), Lei Zhang(张磊), and Li-Yun Jiang(姜立运)

Citation: Chin. Phys. B, 2021, 30 (**6**): 067401. DOI: 10.1088/1674-1056/abdea5
Journal homepage: http://cpb.iphy.ac.cn; http://iopscience.iop.org/cpb

What follows is a list of articles you may be interested in

Quasiparticle interference testing the possible pairing symmetry in Sr_2RuO_4

Cong-Cong Zhang(张聪聪), Jin-Hua Sun(孙金华), Yang Yang(杨阳), Wan-Sheng Wang(王万胜)
Chin. Phys. B, 2020, 29 (**6**): 067401. DOI: 10.1088/1674-1056/ab8888

Josephson effect in the strontium titanate/lanthanum aluminate junction

Xing Yang(阳星), Jie Chen(陈杰), Yabin Yu(余亚斌), Quanhui Liu(刘全慧)
Chin. Phys. B, 2019, 28 (**9**): 097401. DOI: 10.1088/1674-1056/ab33f4

Topological phase diagrams and Majorana zero modes of the Kitaev ladder and tube

Yiming Wang(王一鸣), Zhidan Li(李志聃), Qiang Han(韩强)
Chin. Phys. B, 2018, 27 (**4**): 047401. DOI: 10.1088/1674-1056/27/4/047401

Comparison of band structure and superconductivity in $FeSe_{0.5}Te_{0.5}$ and FeS

Yang Yang(杨阳), Shi-Quan Feng(冯世全), Yuan-Yuan Xiang(向圆圆), Hong-Yan Lu(路洪艳), Wan-Sheng Wang(王万胜)
Chin. Phys. B, 2017, 26 (**12**): 127401. DOI: 10.1088/1674-1056/26/12/127401

Topological phase transition in a ladder of the dimerized Kitaev superconductor chains

Bo-Zhen Zhou(周博臻), Bin Zhou(周斌)
Chin. Phys. B, 2016, 25 (**10**): 107401. DOI: 10.1088/1674-1056/25/10/107401

Temperature and doping dependent flat-band superconductivity on the Lieb-lattice*

Feng Xu(徐峰)[1,2,†], Lei Zhang(张磊)[1,2], and Li-Yun Jiang(姜立运)[1,2]

[1] School of Physics and Telecommunication Engineering, Shaanxi University of Technology, Hanzhong 723001, China
[2] Institute of Graphene at Shaanxi Key Laboratory of Catalysis, Shaanxi University of technology, Hanzhong 723001, China

(Received 10 September 2020; revised manuscript received 10 December 2020; accepted manuscript online 22 January 2021)

We consider the superconducting properties of Lieb lattice, which produces a flat-band energy spectrum in the normal state under the strong electron–electron correlation. Firstly, we show the hole-doping dependent superconducting order amplitude with various electron–electron interaction strengths in the zero-temperature limit. Secondly, we obtain the superfluid weight and Berezinskii–Kosterlitz–Thouless (BKT) transition temperature with a lightly doping level. The large ratio between the gap-opening temperature and BKT transition temperature shows similar behavior to the pseudogap state in high-T_c superconductors. The BKT transition temperature versus doping level exhibits a dome-like shape in resemblance to the superconducting dome observed in the high-T_c superconductors. However, unlike the exponential dependence of T_c on the electron–electron interaction strength in the conventional high-T_c superconductors, the BKT transition temperature for a flat band system depends linearly on the electron–electron interaction strength. We also show the doping-dependent superconductivity on a lattice with the staggered hoping parameter in the end. Our predictions are amenable to verification in the ultracold atoms experiment and promote the understanding of the anomalous behavior of the superfluid weight in the high-T_c superconductors.

Keywords: flat-band superconductivity, strong electron–electron interaction, superfluid weight, Berezinskii–Kosterlitz–Thouless (BKT) transition temperature

PACS: 74.20.−z, 74.20.Mn, 74.25.Bt **DOI:** 10.1088/1674-1056/abdea5

1. Introduction

Flat-band superconductivity has attracted much attention in the condensed matter physics, especially since the recent discovery of superconductivity in flat bands of twisted bilayer graphene.[1–6] A flat band is an energy band without energy dispersion in the quasimomentum $\boldsymbol{k}$ space and is composed of localized eigenstates. In the conventional Bardeen–Cooper–Schrieffer (BCS) theory, the critical temperature of the superconducting transition $T_c \propto \exp\left(-\frac{1}{gn_0(E_F)}\right)$, where g is the coupling constant of attractive interaction and $n_0(E_F)$ is the density of states at the Fermi energy. It is natural to increase the critical temperature by enhancing the density of states which is maximum for the flat band system, because of vanishing the energy dispersion. This might provide a conceivable way to reach the grand goal of room-temperature superconductivity.[7] As the electronic energy band is flat, the momentum uncertainty of the electronic state reaches the maximum, which implies that electrons are more localized in real space according to the uncertainty principle. As a result, the on-site Coulomb interaction is enhanced, so it is necessary to study the flat-band superconductivity that emerges in the strong correlation limit.

Flat bands can be realized in the bipartite lattice, and a simple bipartite lattice featuring a strictly flat band is the Lieb lattice (Fig. 1(a)). It is a line-centered square lattice consisting of three atoms (A, B, C) which tight-binding dispersion is characterized by three band branches, and the middle energy band is a strictly flat band $E_k = 0$.[8] Some theoretical works on the Lieb lattice focus on the ferromagnetic properties; the celebrated flat-band ferromagnetism was first studied by Lieb.[8–11] The studies about superconductivity on the Lieb model show that the high density of states enhances the superconducting critical temperature for fixed interaction strength,[7,12–16] while its topological properties are another interesting topic.[17–20] On the experimental side, the Lieb lattice has been realized using ultracold atoms, photonic lattices and also electronically.[21–23]

Another interesting flat band system is the twisted bilayer graphene. The surprising superconducting state in the twisted bilayer graphene is relevant to flat bands, which arouses new interest in flat-band superconductivity.[1–5,24] There is another simple way to get flat-band superconductivity in graphene by including periodic strain.[25–27] As these systems are two-dimensional, they cannot undergo a conventional phase transition to a superconducting state owing to thermal fluctuation. The superconducting critical temperature is determined by the Berezinskii–Kosterlitz–Thouless temperature rather than the vanishing of the superfluid weight.[28–30,36] Therefore, it is

*Project supported by the National Natural Science Foundation of China (Grant No. 11804213), the Scientific Research Program Funded by Shaanxi Provincial Education Department (Grant No. 20JK0573), the Scientific Research Foundation of Shaanxi University of Technology (Grant No. SLGRCQD2006), and the Natural Science Basic Research Program of Shaanxi (Grant No. 2021JQ-748).

†Corresponding author. E-mail: xufengxlx@snut.edu.cn

© 2021 Chinese Physical Society and IOP Publishing Ltd

crucial to examine the BKT transition on the Lieb model with a strong correlation to understand superfluid in the ultracold atoms or the superconductivity in the high-T_c superconductors.

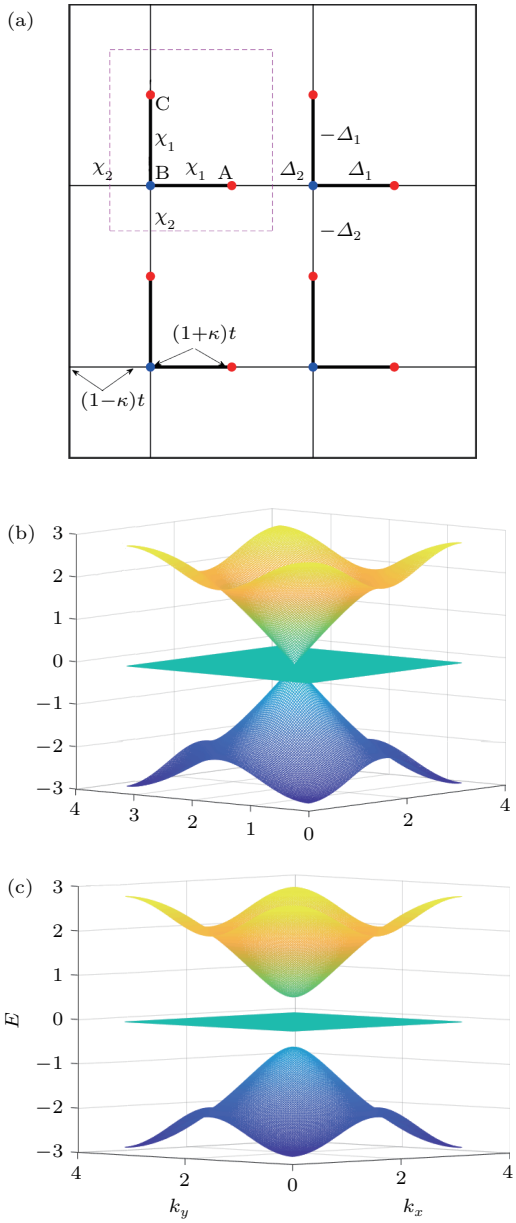


Fig. 1. (a) The Lieb lattice and its unit cell, The sublattice in the unit cell are labeled by $\tau = \mathrm{A,B,C}$. The thick lines represent internal bonds hopping energy $(1+\kappa)t$, while the thin lines represent external bonds hopping energy $(1-\kappa)t$. The mean field parameters χ and Δ used in this paper are set as shown, χ is related to the bond order, Δ is related to the superconducting order, and the d-wave symmetry of the superconducting order is used. (b)–(c) The energy dispersion as a function of quasimomentum for $\kappa = 0$ (b) and $\kappa = 0.2$ (c). The middle band is strictly flat $E_{\boldsymbol{k},0} = 0$ for any κ while the upper and lower band has a gap $E_{\mathrm{gap}} = \sqrt{8}\kappa t$.

In this paper, we investigate the superconducting properties of Lieb lattice in the strong electron–electron correlation limit based on the t–J model using the Gutzwiller renormalization mean-field method. The hole-doping and temperature-dependent superconductivity has been shown. Similar to high-temperature superconductivity in the CuO_2 planes, the superconducting region can be divided into the under-doped region and the over-doped region. The superconducting order amplitude increases linearly with doping level in the lightly doped region in the zero-temperature limit, showing almost irrelevant to electron–electron interaction strength because of the main dependence on the hole-doping level. We obtain the superfluid weight and BKT transition temperature for the d-wave superconducting state on this system. It is shown that the BKT transition temperature is much lower than the gap-opening temperature in the lightly doping level. This phenomenon characterizes the pseudogap state in high-temperature superconductors. As a comparison, the superfluid weight and BKT transition temperature in the optimal hole-doping level have been given. The BKT transition temperature has the same order as the energy gap and superfluid weight disappeared temperature. The BKT transformation temperature versus hole-doping level shows a similar tendency as the doping-dependent superconducting order in the zero-temperature limit. The prominent characteristic in flat-band superconductivity is the linearly increasing relation between superconducting critical temperature and the coupling strength, and we show the BKT transition temperature linearly increases with the electron–electron interaction strength. The effect of the staggered hoping parameter is discussed in the end. It remarkably reduces the superconducting region and the superconducting order in the zero-temperature limit. This paper is organized as follows. In Section 2, we describe the basic theoretical model and Gutzwiller renormalization mean-field method along with the formulation for computing the superfluid weight and the BKT transition temperature. In Section 3, we present our numerical results and discuss their physical meanings. Finally, some conclusions are drawn in Section 4.

2. Model and methodology

We study the extended t–J model on the Lieb lattice (see Fig. 1(a)), governed by the following Hamiltonian:

$$\begin{aligned}
\mathcal{H} = & -\sum_{r_{nm},\sigma}(1+\kappa)t\left(\widehat{b}^{+}_{r_{nm},\sigma}\widehat{a}_{r_{nm}+a\boldsymbol{i},\sigma}+\mathrm{h.c.}\right)\\
& +J_1\left[\widehat{S}_{b_{r_{nm}}}\widehat{S}_{a_{r_{nm}+a\boldsymbol{i}}}-\frac{1}{4}n_{b_{r_{nm}}}n_{a_{r_{nm}+a\boldsymbol{i}}}\right]\\
& -\sum_{r_{nm},\sigma}(1-\kappa)t\left(\widehat{b}^{+}_{r_{nm},\sigma}\widehat{a}_{r_{nm}-a\boldsymbol{i},\sigma}+\mathrm{h.c.}\right)\\
& +J_2\left[\widehat{S}_{b_{r_{nm}}}\widehat{S}_{a_{r_{nm}-a\boldsymbol{i}}}-\frac{1}{4}n_{b_{r_{nm}}}n_{a_{r_{nm}-a\boldsymbol{i}}}\right]\\
& -\sum_{r_{nm},\sigma}(1+\kappa)t\left(\widehat{b}^{+}_{r_{nm},\sigma}\widehat{c}_{r_{nm}+a\boldsymbol{j},\sigma}+\mathrm{h.c.}\right)\\
& +J_1\left[\widehat{S}_{r_{nm}}\widehat{S}_{c_{r_{nm}+a\boldsymbol{j}}}-\frac{1}{4}n_{b_{r_{nm}+a\boldsymbol{i}}}n_{c_{r_{nm}+a\boldsymbol{j}}}\right]\\
& -\sum_{r_{nm},\sigma}(1-\kappa)t\left(\widehat{b}^{+}_{r_{nm},\sigma}\widehat{c}_{r_{nm}-a\boldsymbol{j},\sigma}+\mathrm{h.c.}\right)\\
& +J_2\left[\widehat{S}_{b_{r_{nm}}}\widehat{S}_{c_{r_{nm}-a\boldsymbol{j}}}-\frac{1}{4}n_{b_{r_{nm}}}n_{c_{r_{nm}-a\boldsymbol{j}}}\right], \qquad (1)
\end{aligned}$$

where $\hat{a}_{r_{nm}\sigma}$ ($\hat{a}^{+}_{r_{nm}\sigma}$) annihilates (creates) an electron with spin $\sigma=\uparrow,\downarrow$ on sublattice B of the unit cells located in r_{nm} (an equivalent definition is used for sublattice A and C). The hoping energy of internal bonds in one cell is $(1+\kappa)t$, as well as $(1-\kappa)t$ for external bonds between different cells, the antiferromagnetic coupling $J_1=\frac{4(1+\kappa)^2}{U_1}$ and $J_2=\frac{4(1-\kappa)^2}{U_2}$ with $U_{1/2}$ describes the Hubbard interaction between electrons. The eigenvalues of the noninteracting Hamiltonian of Lieb lattice (with lattice constant a) has three energy bands, and the upper and lower energy band have dispersions

$$E_{\boldsymbol{k},\pm}=\pm 2t\sqrt{1+\kappa^2+(1-\kappa^2)(\cos k_x a+\cos k_y a)/2}, \quad (2)$$

while the middle energy band is strictly flat with $E_{\boldsymbol{k},0}=0$ and isolated from other energy bands with an energy gap $E_{\rm gap}=\sqrt{8}\kappa t$. Unlike the partial loose flat band found in the twisted bilayer graphene, the flat band in this system is strictly $E_{\boldsymbol{k},0}=0$ in the full Brillouin zone.

In the strong interaction limit when U is large, to exclude the doubly occupied state, the effective t–J model is given by $\mathcal{H}_{\rm eff}=P_{\rm G}\mathcal{H}P_{\rm G}$, where $P_{\rm G}=\prod_i\left(1-n_{i\uparrow}n_{i\downarrow}\right)$ is the Gutzwiller projection operator. Following the idea in previous works, we replace the projection operator with the Gutzwiller renormalization factors.[31,32] The hopping amplitude t and the antiferromagnetic coupling J are replaced by $g^t_{ij}t$ and $g^s_{ij}J$ with $g^t_{ij}=g^t_i g^t_j$, $g^t_i=\sqrt{\frac{2\delta_i}{1+\delta_i}}$, $g^s_{ij}=g^s_i g^s_j$, $g^s_i=\frac{2}{(1+\delta_i)}$, where δ_i is the average value of hole-doping level on site i. The antiferromagnetic interaction term $\widehat{S}_i\widehat{S}_j-\frac{1}{4}n_in_j$ has been decoupled as $-\frac{3}{8}\left(\widehat{\chi}^{+}_{ij}\widehat{\chi}_{ij}+\widehat{\Delta}^{+}_{ij}\widehat{\Delta}_{ij}\right)$, where $\widehat{\chi}^{+}_{ij}=\sum_\sigma\widehat{C}^{+}_{i\sigma}\widehat{C}_{j\sigma}$ and $\widehat{\Delta}^{+}_{ij}=\widehat{C}^{+}_{i\uparrow}\widehat{C}^{+}_{j\downarrow}-\widehat{C}^{+}_{i\downarrow}\widehat{C}^{+}_{j\uparrow}$. Taking the mean-field approximation, the mean-field Hamiltonian is given by

$$\mathcal{H}_{MF}=\sum_{\langle i,j\rangle,\sigma}-\left(g^t_{ij}t_{ij}+\frac{3}{8}g^s_{ij}\chi_{ij}\right)\widehat{C}^{+}_{i\sigma}\widehat{C}_{j\sigma}-\frac{3}{8}g^s_{ij}\Delta_{ij}\widehat{\Delta}^{+}_{ij}+\text{h.c.} \quad (3)$$

The chemical potential term $-\mu\widehat{N}$ ($\widehat{N}$ is the particle number operator) is added to get the full Hamiltonian. We defined pair mean field $\Delta_{1/2}$ and bond mean field $\chi_{1/2}$ as follows:

$$\begin{aligned}
\Delta^{\nu}_1&=\frac{1}{N}\sum_{r_{nm}}\langle\widehat{b}_\downarrow(r_{nm})\widehat{a}_\uparrow(r_{nm}+a\boldsymbol{i})-\widehat{b}_\uparrow(r_{nm})\widehat{a}_\downarrow(r_{nm}+a\boldsymbol{i})\rangle,\\
\Delta^{\nu}_2&=\frac{1}{N}\sum_{r_{nm}}\langle\widehat{b}_\downarrow(r_{nm})\widehat{a}_\uparrow(r_{nm}-a\boldsymbol{i})-\widehat{b}_\uparrow(r_{nm})\widehat{a}_\downarrow(r_{nm}-a\boldsymbol{i})\rangle,\\
\chi^{\nu}_1&=\frac{1}{N}\sum_{r_{nm}\sigma}\langle\widehat{b}_\sigma(r_{nm})\widehat{a}_\sigma(r_{nm}+a\boldsymbol{i})\rangle,\\
\chi^{\nu}_2&=\frac{1}{N}\sum_{r_{nm}\sigma}\langle\widehat{b}_\sigma(r_{nm})\widehat{a}_\sigma(r_{nm}-a\boldsymbol{i})\rangle,\\
\delta_{\tau=\rm A,B,C}&=1-\frac{1}{N}\sum_{r_{nm}\sigma}\langle\widehat{\tau}^{+}_\sigma\widehat{\tau}_\sigma\rangle.
\end{aligned} \quad (4)$$

The d-wave superconducting state has been considered in our work, so the mean-field order on the y-direction is considered as shown in Fig. 1(a), and the superscript ν indicates that these quantities are related to the physical order parameters. The superconducting order parameter is given by $\Delta=g^t_{ij}\Delta^{\nu}_{ij}$, and the bond order is also be rescaled. This project is similar to the slave-boson method, where Δ^{ν} equivalents to the average of spinon pairing operators. We perform a discrete Fourier transformation to the mean-field Hamiltonian with

$$\hat{\tau}_{i\sigma}=\frac{1}{N}\sum_{\boldsymbol{k}}\hat{\tau}_{\boldsymbol{k}\sigma}\exp(\mathrm{i}\boldsymbol{k}\cdot\boldsymbol{r}). \quad (5)$$

The mean field Hamiltonian can be then expressed as

$$H_{MF}=\sum_{\boldsymbol{k}}\psi^{\dagger}(\boldsymbol{k})h_{\rm MF}(\boldsymbol{k})\psi(\boldsymbol{k}), \quad (6)$$

where $\psi^{+}=\left(\widehat{a}^{+}_{\boldsymbol{k}\uparrow},\widehat{b}^{+}_{\boldsymbol{k}\uparrow},\widehat{c}^{+}_{\boldsymbol{k}\uparrow},\widehat{a}_{-\boldsymbol{k}\downarrow},\widehat{b}_{-\boldsymbol{k}\downarrow},\widehat{c}_{-\boldsymbol{k}\downarrow}\right)$. Then the mean-field values got by the self-consistent and the temperature-dependence of a mean-field order $\hat{O}$ is obtained by the following equation

$$O(T)=\frac{1}{N}\sum_{\boldsymbol{k}}\langle\hat{O}\rangle=\frac{1}{N}\sum_{n\boldsymbol{k}}\langle\psi_{n\boldsymbol{k}}|\hat{O}|\psi_{n\boldsymbol{k}}\rangle\frac{1}{1+\exp\left(\frac{E_{n\boldsymbol{k}}}{k_{\rm B}T}\right)}, \quad (7)$$

where $\psi_{n\boldsymbol{k}}$ and $E_{n\boldsymbol{k}}$ are the eigenfunction and eigenvalue of the mean-field Hamiltonian, $k_{\rm B}$ is the Boltzmann constant, and T is temperature.

To obtain the superfluid weight, we examine the current response to a vector potential with linear response theory.[33,34] In the presence of the vector potential $A_x(r,t)=A_x(q)\exp(\mathrm{i}qr-\mathrm{i}\omega t)$, the linear current is given by

$$\langle J_x(q,\omega)\rangle=-e^2\left[\langle -K_x\rangle-\Lambda_{xx}(q,\omega)\right]A_x(q,\omega), \quad (8)$$

where $J_x(q,\omega)$ is the total current and Λ_{xx} is the current–current correlation function for the paramagnetic current density. Λ_{xx} is determined by

$$\Lambda_{xx}(q,\mathrm{i}\omega_m)=\frac{1}{N}\int_0^{\beta}\mathrm{e}^{\mathrm{i}\omega_m\tau}\langle J^{\rm P}_x(q,\tau)J^{\rm P}_x(-q,0)\rangle, \quad (9)$$

where $\omega_m=2\pi m^* k_{\rm B}T$ is the Matsubara frequency and is set to $\mathrm{i}\omega_m\to\omega+\mathrm{i}\delta$ in the usual analytic continuation. The paramagnetic current density (x component) at the position r is defined as

$$J^{\rm P}_x(r)=\mathrm{i}t\sum_\sigma(\hat{C}^{\dagger}_{r+x\sigma}\hat{C}_{r\sigma}-\hat{C}^{\dagger}_{r\sigma}\hat{C}_{r+x\sigma}), \quad (10)$$

and the kinetic energy density associated with the x-oriented link at position r is given by

$$\hat{K}(r)=-t\sum_\sigma(\hat{C}^{\dagger}_{r+x\sigma}\hat{C}_{r\sigma}+\hat{C}^{\dagger}_{r\sigma}\hat{C}_{r+x\sigma}). \quad (11)$$

The current–current correlation function is then given by

$$\begin{aligned}
\Lambda_{xx}(q,\mathrm{i}\omega_m)&=\delta\frac{1}{N}\int_0^{\beta}\mathrm{e}^{\mathrm{i}\omega_m\tau}\langle J^{\rm P}_x(q,\tau)J^{\rm P}_x(-q,0)\rangle\\
&=\delta\frac{1}{N}\sum_k J_x(k,q)J_x(-k,-q)\\
&\quad\times\mathrm{Tr}G_0(k+q,i\omega_m+\mathrm{i}\Omega)G_0(k,\mathrm{i}\Omega)(-1)\\
&=\delta\frac{t^2}{N}\sum_{k,n,m}U^{\dagger}(k)\Xi U(k+q)U^{\dagger}(k+q)\Xi U(k)
\end{aligned}$$

$$\times \frac{f(E_n(k+q)) - f(E_m(k))}{E_n(k+q) - E_m(k) + \mathrm{i}\omega_m}, \tag{12}$$

where $U(k) = (\psi_{1k}, \psi_{2k}, ..., \psi_{nk})$, ψ_{nk} is the eigenstate of the mean-field Hamiltonian, Ξ is the matrix form of J_x, $f(E_n)$ is the Fermi–Dirac distribution function, and δ is the hole-doping level. The superfluid weight D_s is then obtained by setting

$$\frac{D_s(T)}{\pi e^2} = \langle -K_x \rangle - \Lambda_{xx}(q_x = 0, q_y \to 0, \mathrm{i}\omega_m = 0) \equiv \frac{n_s(T)}{m^*}, \tag{13}$$

with the restricted condition $\langle -K(x) \rangle - \Lambda_{xx}(q_x \to 0, q_y = 0, \mathrm{i}\omega_m = 0) = 0$ as required by gauge invariance. Here the superfluid density $n_s(T)$ is determined through the superfluid weight as $n_s(T) = m^* \frac{D_s}{\pi e^2}$ with m^* being the effective mass for the Cooper pair. The doping effect has been included similar to the superfluid weight formula in the slave-boson mean field theory introduced in the previous work.[35] As the system is two-dimensional, the critical temperature transition to superconductivity is determined by the BKT transition temperature as

$$k_B T_{BKT} = \frac{\pi \hbar^2}{8} \frac{n_s(T_{BKT})}{m^*}. \tag{14}$$

Since the superfluid density $n_s(T)$ is obtained by numerical calculating, it is equivalent to the definition in terms of the stiffness of the superconducting order parameter in the thermodynamic potential.

3. Results and discussion

As mentioned above, we can achieve the strong constraint of forbidding double occupancy of two electrons on the same site using Gutzwiller factors, then study the superconducting properties of Lieb-Lattice on the mean field level. In our work, the pair field Δ^{ν} represents the local electron pairing order, and bond order χ^{ν} is the kinetic hopping term. We first show the superconducting order amplitude versus hole-doping level in the zero-temperature limit with various electron–electron coupling strengths in Fig. 2. Here we choose $\kappa = 0$, which shows no energy gap between the upper and lower energy band in the normal state and the mean field values $\Delta_1^{\nu} = \Delta_2^{\nu}$, $\chi_1^{\nu} = \chi_2^{\nu}$ according to the symmetry. There are two distinct regions for different hole-doping levels analogous to hole-doped dependent in the high-temperature superconductivity in the CuO_2 planes. The physical superconducting order linearly increases with the hole-doping level δ for various electron–electron coupling strengths in the under-doped region. The doping level δ is defined as $\delta = \delta_A + \delta_B + \delta_C$; when $\delta = 0$, the flat band is half filled, and when $\delta = 1$, the flat band is empty. The superconducting order amplitude mainly depends on the hole-doping level, so there is almost no difference with various electron–electron coupling strengths. The optimum doping level increases with the effective attraction strength between electrons and the maximum value of superconducting order. The superconducting region conspicuously reduces with the enhancement of the Hubbard interaction U, and the superconducting order rapidly declines with the doping level in the over-doped region. In particular, it should be noted that the superconducting order includes the contributions from all energy bands; however, the middle flat energy band plays an essential role.

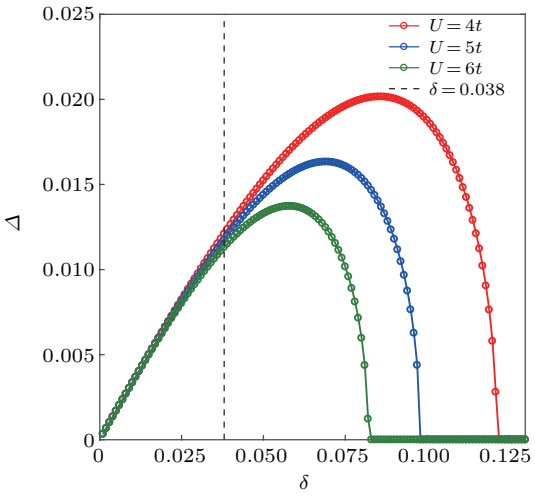


Fig. 2. The superconducting order near-zero temperature varies with the hole-doping level δ, and $\kappa = 0$ shows no energy gap between the upper and lower energy band in the normal state. The superconducting order is dominated by the hole-doping level when $\delta \leq 0.038$, and they linearly increase with δ with various Hubbard interaction U. Up to a maximum value, the superconducting order increases with the doping level, after that, rapidly decreases with it. The superconducting region decreases with the effective attraction strength $J = 4t^2/U$ between pair electrons.

The enigmatic pseudogap state in high-temperature superconductors has long been recognized as a central puzzle in the research of cuprate superconductivity. It is widely proved that the pseudogap opens below a temperature much above the superconducting transition temperature in the under-doped region. We obtain the superfluid weight and BKT transition temperature with the help of linear response theory. The temperature-dependent physical orders in the lightly doping level $\delta = 0.03$ with $\kappa = 0, U = 4t$ are shown in Fig. 3(a), and the superconducting order Δ decreases with temperature increasing. In Fig. 3(b), we show the superfluid weight as a function of temperature and get the BKT transition temperature. It is found that the superfluid weight decreases almost linearly with temperature due to the quasi-particles energy spectrum being gapless. The BKT transition temperature is determined by the intersection of $\hbar^2 n_s(T)/m^*$ with $8k_B T/\pi$. The BKT transition is noteworthy lower than the temperature of the superfluid weight disappearance. As shown in Fig. 3, the gap opening temperature T^* is much higher than the superconducting critical temperature T_{BKT} with ratio $T^*/(T_{BKT}) \approx 10$. The considerable disparity between T^* and T_{BKT} is similar to the pseudogap state in the high-temperature cuprate superconductors and may be used to understand the anomalous behavior of the superfluid weight in the high-T_c superconductors. The status for the optimum doping level $\delta = 0.086$ with $U = 4t, \kappa = 0$

has been shown in Fig. 4 as a comparison. The critical temperature of the superconducting order is almost equal to the temperature of the superfluid weight disappearance.

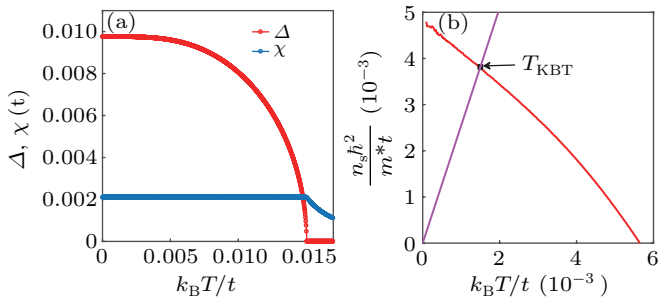


Fig. 3. (a) The superconducting order and the bond order evolution as a function of temperature at the lightly hole-doping level $\delta = 0.03, U = 4t, \kappa = 0$. (b) The superfluid weight decreases with the temperature and the BKT transition temperature point.

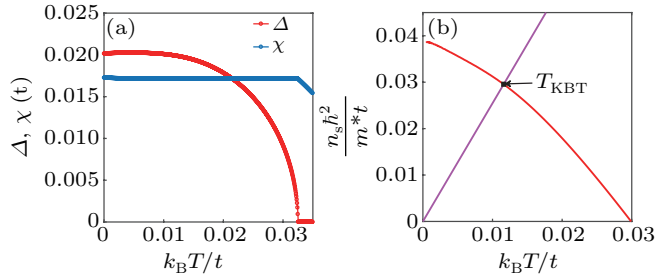


Fig. 4. (a) The superconducting order and the bond order evolution as a function of temperature at the optimal hole-doping level $\delta = 0.086, U = 4t, \kappa = 0$. (b) The superfluid weight decreases with the temperature and the BKT transition temperature point.

The BKT transition temperature versus the hole-doping level δ is shown in Fig. 5(a). Clearly, it exhibits a dome-like shape in resemblance to the superconducting dome observed in the high-T_c cuprate superconductors and a recent similar situation discovered in the twisted bilayer graphene. The superconductivity emerges from $\delta = 0.01$, the BKT transition temperature near zero under this doping level, and there is no physical realistic superconducting state under this condition. It is in accord with the consensus that there is no superconductivity in a strong correlation system near the half-filled. The superconducting critical temperature T_{BKT} increases with the doping level in the under-doped region, while it decreases with the doping level in the over-doped region. The flat-band superconductivity in this system is very different from other flat band systems; its superconducting region with hole-doping level is much smaller than twisted bilayer graphene and strained graphene. This significant difference is caused by the strong ferromagnetic fluctuation on the Lieb lattice even under hole doping; however, the magnetic fluctuation in the twisted bilayer graphene and strained graphene is suppressed rapidly with the increase of the hole-doping level. As shown in Fig. 5(b), The BKT transition temperature linearly increases with the effective electron–electron attractive interaction $J = 4t^2/U$ for the strong Hubbard interaction from $U = 4t$ to $U = 6t$. The linear relationship between T_{BKT} and J is a characteristic of the flat-band superconductivity in contrast to the relation for the critical temperature $T_c \sim e^{-1/g}$ in the conventional superconductors. Even in the presence of the strong and repulsive correlation effect, the flat-band superconductivity is a potential route to high-temperature superconductivity.

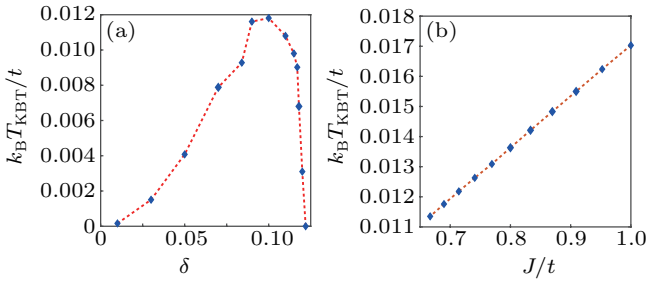


Fig. 5. (a) The BKT transformation temperature versus hole-doping level δ with $U = 4t, \kappa = 0$. (b) The BKT transition temperatures linearly increase with the coupling constant with $\delta = 0.06$, $\kappa = 0$, $U = 4t$ to $6t$.

Finally, we discuss the staggered effect in the lattice with the staggered hoping parameter on the superconducting state in the zero-temperature limit. Clearly, the superconducting region remarkably dwindles with $\kappa = 0.2$. The main relationship between the superconducting order and the doping level is the same as the symmetry condition ($\kappa = 0$); however, the superconducting state disappears with the maximal doping level $\delta = 0.029$. The superconducting order is much smaller than the symmetry case with three orders of magnitude as shown in Fig. 6, and the staggered hoping parameter makes the mean field value $\Delta_1 \neq \Delta_2$, $\chi_1 \neq \chi_2$. The superconducting state on the staggered Lieb lattice is restricted and hard to realize.

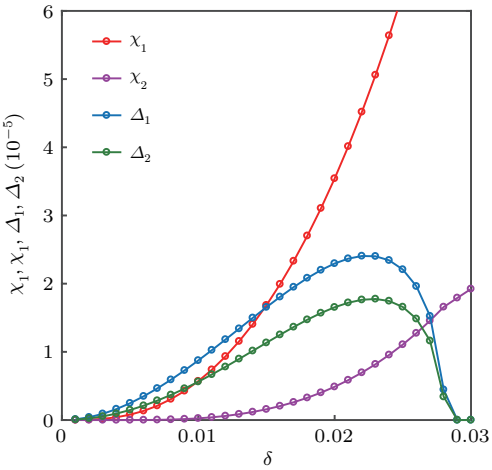


Fig. 6. The superconducting order and the bond order in the zero-temperature limit versus the hole-doping level δ with staggered hopping parameters $\kappa = 0.2, U = 4t$.

4. Conclusion

In summary, we have shown the d-wave superconducting state on the Lieb lattice with a flat-band spectrum in the normal state in the strong electron–electron correlation limit. The superconducting order amplitude mainly depends on the hole-doping level and increases with it for various electron–electron coupling strengths in the lightly doped region, but

rapidly decreases with doping level after reaching its maximum value. The hole-doping dependent superconducting properties of Lieb lattice are similar to the case in the cuprate superconductors. We study the thermal behavior of superfluid weight and get the BKT transition temperature which is used as the superconducting critical temperature because this system is two-dimensional. The conspicuous difference between gap opening temperature T^* and $T_{\rm BKT}$ in the under-doped region is helpful to understand the enigmatic pseudogap state in the high-temperature superconductors. The dome-like shape of the BKT transition temperature versus hole-doping level is shown in resemblance to the superconducting dome observed in the high-$T_{\rm c}$ cuprate superconductors and twisted bilayer graphene. The BKT transition temperature depends linearly on the electron–electron interaction strength, which shows the flat band plays a dominant role in the superconducting state on the Lieb lattice. The staggered effect on the lattice remarkably reduces the superconducting region. Lastly, a highly tunable Lieb lattice can be realized with ultracold gases in the experiment, and our results can examine and promote the understanding of the anomalous behavior of the superfluid weight in the high-$T_{\rm c}$ superconductors. The flat-band ferromagnetism brings strong ferromagnetic fluctuation on the Lieb lattice even under hole doping, so we will consider the ferromagnetic effect on the superconductivity under strong electron–electron correlation in future work.

Acknowledgement

We thank professor C. Y. Mou for the fruitful discussions.

References

[1] Cao Y, Fatemi V, Fang S, Watanabe K, Taniguchi E, Kaxiras E and Jarillo-Herrero P 2018 *Nature* **556** 43
[2] Chebrolu N R, Chittari B L and Jung J 2019 *Phys. Rev. B* **99** 235417
[3] Hu X, Hyart T, Pikulin D I and Rossi E 2019 *Phys. Rev. Lett.* **123** 237002
[4] Roy B and Juricic V 2019 *Phys. Rev. B* **99** 121407(R)
[5] Julku A, Peltonen T J, Liang L, Heikkila T T and Torma P 2020 *Phys. Rev. B* **101** 060505(R)
[6] Kopnin N B, Heikkila T T and Volovik G E 2011 *Phys. Rev. B* **83** 220503(R)
[7] Iglovikov V I, Hebert F, Batrouni G G and Scalettar R T 2014 *Phys. Rev. B* **90** 094506
[8] Lieb E H 1989 *Phys. Rev. Lett.* **62** 1201
[9] Mielke A 1991 *J. Phys. A* **24** L73,1991 *J. Phys. A* **24** 3311
[10] Tasaki H 1992 *Phys. Rev. Lett.* **69** 1608
[11] Tasaki H 1998*Prog. Theor. Phys.* **99** 489
[12] Kopnin N B, Heikkila T T and Volovik G E 2011 *Phys. Rev. B* **83** 220503(R)
[13] Wang H, Yu S L and Li J X 2014 *Phys. Lett. A* **378** 3360
[14] Julku A, Peotta S, Vanhala T I, Kim D H and Torma P 2016 *Phys. Rev. Lett.* **117** 045303
[15] Huhtinen K F,Tylutki M, Kumar P, Vanhala T I, Peorra S and Torma P 2018 *Phys. Rev. B* **97** 214503
[16] Tylutki M and Torma P 2018 *Phys. Rev. B* **98** 094513
[17] Sun K, Gu Z, Katsura H and Sarma S D 2011 *Phys. Rev. Lett.* **106** 236803
[18] Tang E, Mei J W and Wen X G 2011 *Phys. Rev. Lett.* **106** 236802
[19] Neupert T, Santos L, Chamon C and Mudry C 2011 *Phys. Rev. Lett.* **106** 236804
[20] Roy R 2014 *Phys. Rev. B* **90** 165139
[21] Slot M R, Gardenier T S, Jacobse P H, van Miert G C P, Kempkes S N, Zevenhuizen S J M, Smith C M, Vanmaekelbergh D and Swart I 2017 *Nature Physics* **13** 672
[22] Lin Z, Choi J H, Zhang Q, Qin W, Yi S, Wang P, Li L, Wang Y, Zhang H, Sun Z, Wei L, Zhang S, Guo T, Lu Q, Cho J H, Zeng C and Zhang Z 2018 *Phys. Rev. Lett.* **121** 096401
[23] Xia S, Ramachandran A, Xia S, Li D, Liu X, Tang L, Hu Y, Song D, Xu J, Leykam D, Flach S and Chen Z 2018 *Phys. Rev. Lett.* **121** 263902
[24] Saito Y, Ge J, Watanabe K, Taniguchi T and Young A F 2018 *Nature Physics* **14** 3681
[25] Kauooila V J, Aikebaier F and Heikkila T T 2016 *Phys. Rev. B* **93** 214505
[26] Xu F, Chou P, Chung C H, Lee T K and Mou C Y 2018 *Phys. Rev. B* **98** 205103
[27] Xu F and Zhang L 2019 *Chin. Phys. B* **28** 117403
[28] Berezinskii V L 1972 *Sov. Phys. JETP* **34** 610
[29] Kosterlitz J M and Thouless D J 1973 *J. Phys. C* **6** 1181
[30] Nelson D R and Kosterlitz J M 1977 *Phys. Rev. Lett.* **39** 1201
[31] Lee P A, Nagaosa N and Wen X G 2006 *Rev. Mod. Phys.* **78** 17
[32] Edegger B, Muthukumar V N and Gros C 2007 *Adances in Physics* **56** 927
[33] Scalapino D J, White S R and Zhang S C 1992 *Phys. Rev. Lett.* **68** 2830
[34] Scalapino D J, White S R and Zhang S C 1993 *Phys. Rev. B* **47** 7996
[35] Zhong Y, Lu H and Luo H 2016 *Eur. Phys. J. B* **89** 28
[36] Shao S, Zhou K and Zhang Z 2019 *Chin. Phys. B* **28** 070501